

2015

## CHARACTERIZATION OF ELECTRODEPOSITED POLYANILINE BIOSENSOR PLATFORM FOR ESCHERICHIA COLI O157:H7 DETECTION

Sterling Prince  
*Michigan Technological University*

Follow this and additional works at: <https://digitalcommons.mtu.edu/etds>



Part of the [Electrical and Computer Engineering Commons](#)

Copyright 2015 Sterling Prince

---

### Recommended Citation

Prince, Sterling, "CHARACTERIZATION OF ELECTRODEPOSITED POLYANILINE BIOSENSOR PLATFORM FOR ESCHERICHIA COLI O157:H7 DETECTION", Master's report, Michigan Technological University, 2015.  
<https://doi.org/10.37099/mtu.dc.etds/895>

Follow this and additional works at: <https://digitalcommons.mtu.edu/etds>



Part of the [Electrical and Computer Engineering Commons](#)

CHARACTERIZATION OF ELECTRODEPOSITED POLYANILINE BIOSENSOR  
PLATFORM FOR ESCHERICHIA COLI O157:H7 DETECTION

By

Sterling Prince

A REPORT

Submitted in partial fulfillment of the requirements for the degree of

MASTER OF SCIENCE

In Electrical Engineering

MICHIGAN TECHNOLOGICAL UNIVERSITY

2015

© 2015 Sterling Prince

This report has been approved in partial fulfillment of the requirements for the Degree of  
MASTER OF SCIENCE in Electrical Engineering

Department of Electrical and Computer Engineering

Report Advisor: *Paul L Bergstrom*

Committee Member: *Adrienne R Minerick*

Committee Member: *Keat G Ong*

Department Chair: *Daniel R Fuhrmann*

## Dedication

To my mother, my father, and my family and above all Almighty God who deserves all the glory.

# Table of Contents

<b>1. Introduction</b> .....	8
1.1 IMPORTANCE OF ESCHERICHIA COLI O157:H7 DETECTION.....	8
1.2 APPLICATION OF CONDUCTIVE POLYMERS TO SILICON NANOWIRES .....	9
1.3 RESEARCH OBJECTIVE.....	10
<b>2. Experiment and Characterization</b> .....	11
2.1 SCALABLE TEST DEVICE PROCESS FLOW.....	11
2.1.1 Design constraints.....	11
2.1.2 Device fabrication and process flow.....	12
2.2 ELECTRODEPOSITION TESTING AND CHARACTERIZATION METHODS.....	14
2.2.1 Experimental materials and methods.....	14
2.2.2 Constant current source method.....	15
2.2.3 Ellipsometric film characterization.....	16
2.2.3.1 Thickness.....	16
2.2.3.2 Uniformity.....	17
2.2.3.3 Repeatability.....	17
2.3 IMMOBILIZING ANTI ESCHERICHIA COLI ON POLYANILINE SURFACE.....	17
2.3.1 Experimental materials and method.....	18
2.3.1.1 Avidin immobilization on polyaniline surface.....	18
2.3.1.2 Anti-Escherichia coli O157:H7 biotinylation process .....	21
2.3.1.3 Anti-Escherichia coli O157:H7 immobilization .....	23
<b>3. Results and Discussion</b> .....	24
3.1 CHALLENGES ENCOUNTERED DURING ELECTRODEPOSITION PROCESS.....	24
3.1.1 Current density challenges.....	24
3.1.2 Importance of clean electrodes.....	24
3.1.3 Film saturation.....	25
3.2 ELLIPSOMETRIC CHARACTERIZATION OF POLYANILINE.....	25
3.2.1 Modeling polyaniline films using Cauchy equation.....	25

3.2.2 Modeling polyaniline films using Cauchy-Urbach equation.....	26
3.2.3 Thickness results.....	29
3.2.4 Uniformity results.....	30
3.2.5 Repeatability results.....	32
3.2.6 Ellipsometric challenges with large angle measurements.....	34
3.3 IMMOBILIZING ANTI ESCHERICHIA COLI ON POLYANILINE SURFACE RESULTS.....	34
3.3.1 Verifying avidin protein crosslinking with polyaniline.....	34
3.3.1.1 Ellipsometric surface thickness change results.....	34
3.3.1.2 FTIR spectroscopy results.....	36
3.3.2 Verifying antibody immobilization with polyaniline.....	38
3.3.2.1 Raman spectroscopy results.....	38
3.3.2.2 Fluorescence microscopy results.....	41
<b>4. Conclusion.....</b>	<b>44</b>
<b>5. Future Work.....</b>	<b>44</b>
5.1 ELECTRODEPOSIT USING CYCLIC VOLTAMMETRY METHOD .....	44
5.2 OPTIMIZE CHEMICAL PROCESS TO INCREASE ANTIBODY DENSITY.....	44
5.3 REDUCE AVIDIN CONCENTRATION.....	45
5.4 INVESTIGATE AVIDIN BIOTIN COMPLEX ONLY.....	45
<b>6. References.....</b>	<b>46</b>

## Acknowledgements

The author is grateful to Dr. Paul Bergstrom and the Microfabrication Facility(MFF) at Michigan Technological University for the guidance, support, and funding of this work. The author gratefully acknowledges Dr. Adrienne Minerick and her research group for working alongside him, allowing him to use their facilities, and the many interesting group discussions. The author is also appreciative of Dr. Yoke Kin Yap's research group for their help with Raman spectroscopy and FTIR studies. The author would also like to thank Dr. Caryn Heldt for providing technical information regarding the chemistries used for binding the antibody used in this work and for providing support with understanding experimental results. The author wants to express a sincere thanks to Shiva Bhandari, Nupur Bihari, Thomas Daunais, and Zhichao Wang for their help throughout the experimental process.

## Abstract

Amperometric electrodeposition has been used to obtain uniform, conductive, and repeatable polyaniline (PANi) thin films for use in nano scaled biochemical sensors. This report describes the characterization of these films. Techniques such as ellipsometry was used to test repeatability of the deposition and the uniformity of the deposited thin films. Raman spectroscopy was utilized to confirm the composition of the deposited PANi thin films. Fluorescence microscopy was used to determine the immobilization of antibodies to the PANi thin films using biotin-avidin interactions, as well as the density of active binding sites. Ellipsometry results demonstrated that biomolecules could be immobilized on PANi films as thin as 9nm. Evidence from the Raman spectroscopy demonstrated the conductive nature of the PANi films. The fluorescence microscopy demonstrated that antibodies could be immobilized on PANi films, although the experiment also demonstrated a low density of binding sites. The characterization demonstrates the utility of the PANi thin films as a conductive interface between the inorganic sensor platform and biochemical molecules.



# 1. Introduction

## 1.1 IMPORTANCE OF ESCHERICHIA COLI O157:H7 DETECTION

According to the Center for Disease Control and Prevention(CDC) the escherichia coli(*E. coli*) bacteria that produce a toxin named shiga toxin(STEC) are estimated to cause 265,000 STEC infections to people in the United States each year. Of these infections, *E. coli* O157:H7 is responsible for 36% of the infections[1]. Over the last 5 years the United States has seen outbreaks related to this type of bacteria in foods such as cheese, ground beef, ready to eat salads and frozen food products[2]. Health issues associated with this bacterial pathogen have ranged from mild problems such as headache and fever to more serious problems such as bloody diarrhea and a life threatening kidney problem known as hemolytic uremic syndrome[1, 3]. To reduce the number of people who get sick, become hospitalized, or die from this foodborne pathogen researchers are focusing on developing better preventative sensor technology to quickly identify the pathogen. The benefits of prompt diagnosis of STEC infection can help in mitigating further complications to the exposed person such as preventing renal failure and avoiding unnecessary treatments such as surgeries for patients with severe abdominal pains[4, 5]. Timely diagnosis of the STEC pathogen can also help in the detection of outbreaks and in reducing the spread of the infection in public places such as food services, nursing homes, and childcare settings[4].

The traditional diagnostic method performed to test for *E. coli* O157:H7 consist of testing the stool sample of an infected person in a public or clinical laboratory by culturing the stool specimen on a sorbitol selective medium[6]. The STEC pathogen can be effectively distinguished from other generic *E. coli* pathogens by its inability to ferment sorbitol during this culturing process [4, 6, 7]. Although the culturing method is commonly used for detecting the O157 STEC, the length of time associated with the method to identify the pathogen can take up to 24 hours [6].

A non-culture diagnostic method such as polymerase chain reaction(PCR) is also used to detect specific genes that encode the toxin(stx1 and stx2)[4]. The sensitivity of this method is low when used on DNA extracted from direct stool samples[4]. As a result, a subculture in an enrichment broth is prepared to increase the sensitivity[4]. The PCR enrichment broth process takes an average of 24 to 36 hours for the verification[4]. Although, the PCR method is selective enough to distinguish between specific genes, the method involves many screening steps and is said to be a labor extensive and time consuming procedure[6, 7].

Shiga toxin enzyme immunoassays are another diagnostic method used to identify *E. coli* O157. The test for the shiga toxin using this method is not directly performed on the

primary stool sample due to the small quantity of bacteria present in stools[4]. Instead an enrichment broth culture is prepared overnight(16-24h) and this culture is tested for the E. coli O157 pathogen[4]. The sensitivity and specificity of these immunoassays are said to differ by manufacturer. While shiga toxin enzyme immunoassays are beneficial for diagnostic identification purposes, it is noted that culturing methods are currently still needed because culturing provides isolation of the pathogen which is important for serotyping. Furthermore, culturing allows the added benefit of characterizing the STEC to determine the specific severity of the pathogen. It was summarized that the best strategy to be used in detecting E. coli O157 would be to culture the stool while simultaneously testing for shiga toxin to insure complete detection and serotyping[4].

Since challenges exist with the current methods of detecting E. coli O157, biosensors are being explored to address and overcome these challenges. A significant effort is being focused on creating biosensors which have high sensitivity and selectivity to E. coli O157:H7 [3, 8], a cost effective manufacturing process[3, 9], and can quickly identify the food pathogen with label free recognition[9, 10].

## **1.2 APPLICATION OF CONDUCTIVE POLYMER TO SILICON NANOWIRES**

The investigator's research group has specialized in research involving silicon nanowires(SiNWs) characterization and fabrication methods to produce top down SiNWs for food pathogen detection. SiNWs have been found to be well suited for high sensitivity detection because they can be fabricated to have a high surface area to volume ratio[11]. This property allows for small changes on the surface of the nanowire to have large impacts on the impedance of the device, giving the device high sensitivity to femtomolar concentrations of analyte and below[12]. A few other groups researching nanowires(NWs) provide supportive results that predict that as NWs become smaller, their sensitivity may increase enough for them to be able to detect single molecule events[11, 13]. However, the drawback of reducing the size of NWs is that the technologies used to fabricate NWs, such as electron beam lithography, is still very expensive and not suitable for large scale manufacturing[11].

Ultra-thin conductive polymers electrodeposited onto the surface of biosensor transducers have found various uses over recent years in biosensing applications. The conductive polymer layer is said to provide the ability to efficiently transfer the electric charges produced by biochemical reactions to the electronic circuit[14]. In addition, electrodeposited conductive polymers provide a controlled method of trapping biologically active molecules in the film which is useful in creating bioelectrodes with localized functionalization[15]. In particular, the polymer polyaniline (PANi) has been widely used as a polymer for biosensing applications. It also stands out among other conductive polymers for the use in biosensors

because it is biocompatible, easy to synthesize, can be doped to change its conductive properties, and has excellent biochemical and thermal stability[13, 16]. The nanostructured form of PANi was reported as having a high surface to volume ratio which would be useful in the immobilization of a greater amount of biomolecules[16]. Furthermore, with the ability to incorporate a greater amount of biomolecule, it was reported that biosensors with PANi coatings would have enhancements in sensitivity and response time[16]. The present work in this paper describes the integration of the silicon nanowire technology, conductive polymer polyaniline and biotin-avidin based biomolecule immobilization technique with the motivation for detecting E. coli O157:H7 pathogen from this combined biosensing platform to achieve enhanced sensitivity and specificity.

### **1.3 RESEARCH OBJECTIVE**

This research study focuses on the design and development of a technique to immobilize and detect fluorescence tagged anti Escherichia O157:H7 on the surface of an electrodeposited polyaniline-silicon substrate.

Specific objectives:

1. To fabricate a controllable device platform for experimental film deposition.
2. To obtain a repeatable process for electrodepositing polyaniline films on *p*+ -doped silicon.
3. To obtain a process to modify polyaniline surface to accept antibodies.
4. To identify and use an imaging technique to confirm the existence of antibodies bound to polyaniline surface.

## 2. Experiment and Characterization

### 2.1 SCALABLE TEST DEVICE PROCESS FLOW

Prior research with bare oxide surface silicon nanowire FET devices showed a need for improvement in the surface oxide-biological solution interface. Conductive polymer polyaniline was chosen as an alternative to having an oxide layer on the surface of the nanowire to improve the conductive properties of the nanowire FET and take advantage of antibody immobilization on the surface of the polymer for specific biomolecule detection. The understanding of how electrodeposited polyaniline behaved for a  $p+$  silicon nanowire was studied using a larger test area, where results could be appropriately scaled down to eventually use the film on nanowire silicon surfaces. In this section of the report, the details pertaining to the fabrication of an approximately  $645 \text{ mm}^2$  square silicon substrate test device is described. Each of these samples contain two circular openings of exposed  $p+$  silicon, while the rest of the sample has photoresist masking it. Each silicon opening measures 3.5 mm in diameter with an area of  $9.62 \text{ mm}^2$ . This circular region is used as the working area to electrodeposit polyaniline films.

#### 2.1.1 Design constraints

It was a necessity to have certain design parameters held constant in the device.

1. A heavily doped substrate with a doping of  $10^{19} \text{ cm}^{-3}$  was used to increase conductive behavior.
2. Control of the area exposed to solution was required. The amount of substrate area exposed to solution needed to be controlled. This would insure the same current density was used in each experimental trial.
3. A hydrofluoric acid(HF) resistant layer needed to surround the exposed deposition area. This barrier protected the integrity of the device against a 20 sec HF surface activation step.
4. An electroplating working area large enough to be analyzed by the beam size of an Ellipsometer.
5. A contact pad on the top of the test device that would connect it to the working electrode.

### 2.1.2 Device fabrication and process flow

In this section the steps involved in the development of the scalable device for polyaniline electrodeposition is explained in detail. A visual schematic detailing the design and fabrication steps involved is provided below for further clarification.

A batch of heavily doped, 100mm diameter silicon <100> substrates were acquired. A thermal oxide was grown on the silicon wafers in a furnace at 1000°C in O<sub>2</sub> with a final thickness measuring of 80 nm. Positive photoresist, Futurrex PR1-1000A, was applied in a spin process over the oxide layer. Photolithography was used to pattern circles with a diameter of 3.5 mm and an area of 9.62 mm<sup>2</sup> across the wafer. After development, the 9.62 mm<sup>2</sup> circular windows were opened. A 10:1 buffered solution of hydrofluoric acid was used to etch the exposed oxide layer in the circular openings. A reactive sputtered nitride from a silicon target was deposited on the back side of the wafer. The wafer was then cleaved into square pieces measuring approximately 1.5 mm x 3 mm in width and length respectively. Approximately 13 mm of the top side of each square piece was submerged in acetone followed by a dip in buffered hydrofluoric acid.(See figure 2.1)

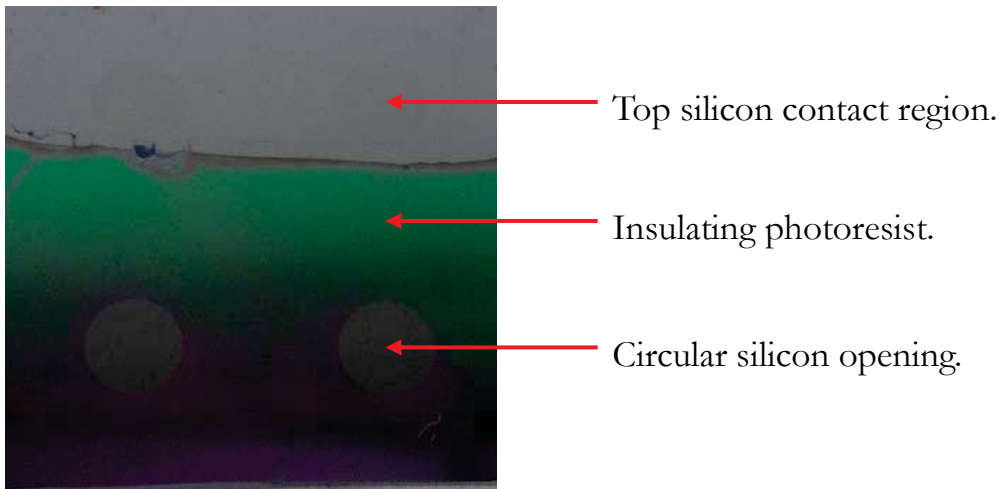


**Figure 2.1 Scalable test device sample with two 9.62 mm<sup>2</sup> circular p+ Si openings.**

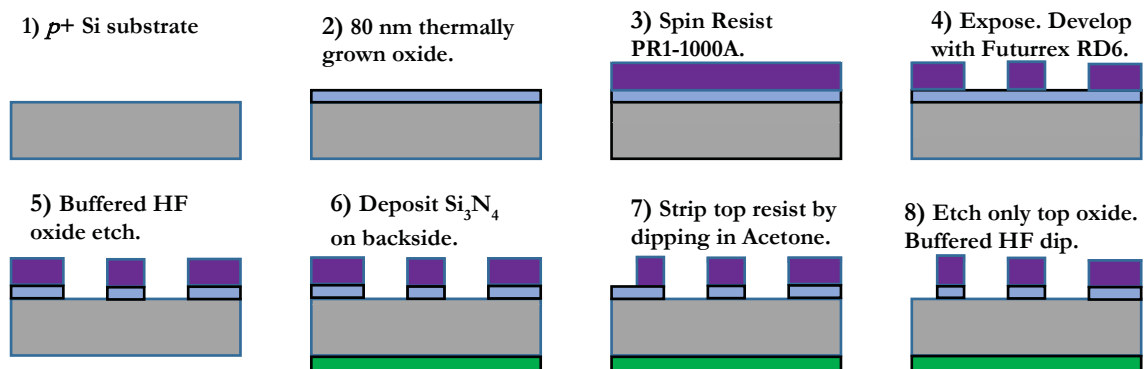


**Figure 2.2 Cross sectional view of the process flow for the scalable test device.**

- a. Heavily doped silicon 100 mm diameter silicon <100> substrates were acquired.
- b. 80nm thermal oxide was grown on top of silicon substrate at a temperature of 1000°C in O<sub>2</sub> for 90 minutes.
- c. Positive photoresist Futurrex PR1-1000A was spun over oxide for 40 sec at 3000 rpm.
- d. Bake substrate on hot plate at 120°C for 120 sec.
- e. Expose for 12 sec on EV620 contact aligner. (Mask 3.5mm diameter circular openings)
- f. Develop with Futurrex RD6 for 10 sec.
- g. Submerge wafer in 10:1 buffered hydrofluoric acid for 40 sec.
- h. Rinse in DI water and dry with nitrogen.
- i. Deposit a 50 nm silicon nitride film through reactive nitride sputtering on *backside* of wafer from a silicon target in the Perkin Elmer 2400-8J RF sputter deposition system in N<sub>2</sub>.
- j. Cleave the wafer into 645 mm<sup>2</sup> square pieces.
- k. Remove 13 mm of photoresist from one end of the square piece by dipping it into acetone.
- l. Remove 13 mm of the exposed oxide layer from the same end of the square piece that was previously dipped in acetone by submerging it in 10:1 buffered hydrofluoric acid solution for 45 sec.
- m. Rinse in DI water and dry with nitrogen.

## 2.2 ELECTRODEPOSITION TESTING AND CHARACTERIZATION METHODS

### 2.2.1 Experimental materials and methods

#### Chemicals

Aniline, Ammonium Fluoride, Hydrofluoric acid, Hydrochloric acid. Solutions were prepared in deionized water.

#### Experimental Setup

The electrochemical process was adapted and optimized from a polyaniline deposition sequence described in literature by A. Deep et al[16].

Instead of a three electrode electrochemical configuration, the studies here were operated in a two electrode configuration forgoing an isolated reference electrode and using the counter electrode also as the reference electrode for the solution. The working electrode was connected to the top edge of the fabricated test device. A platinum wire was used as the counter electrode. The experiments were conducted in an aniline solution prepared with a concentration 0.1M in 1M HCl[16]. 150 ml of the prepared aniline solution was poured into a glass beaker in which the experiment would take place. Each experimental run required that the circular silicon openings in the test device to become H-terminated silicon surfaces before running the electrochemical process. This entailed an initial step of dipping the silicon circular openings in 10:1 hydrofluoric acid for 20 sec followed by a 4 minute submergence of the circular openings in ammonium fluoride[16]. The test device was then removed from the ammonium fluoride and mounted onto an adjustable Teflon turret and lowered into the aniline solution. Figure 2.3 illustrates a simple view of the experimental setup used in the electrodeposition process.

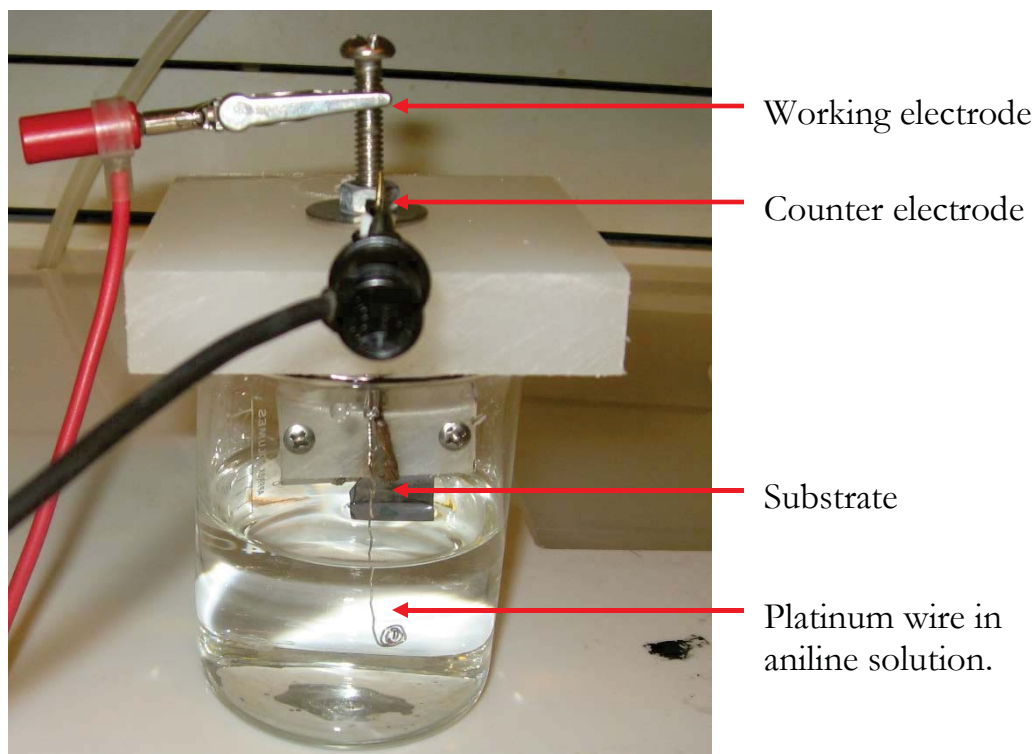


**Figure 2.3 Simple view of the electrodeposition experimental setup.**

### 2.2.2 Constant current source method

A Keithley 2400 Sourcemeter was used to provide a constant current to the working electrode while conducting the electrodeposition experiment. The exposed top surface of the test device was made to contact the working electrode while the silicon circular openings were submerged in the aniline solution. A platinum counter electrode was held at a fixed distance of 25 mm away from the working electrode in the aniline solution. Experiments were carried out by applying a constant current to the working electrode and performing the electrodeposition for a fixed time. During the electrodeposition process, the aniline is attracted to the working electrode and deposits on the conducting silicon in the two 3.5 mm diameter circular openings. After the deposition takes place, the sample is removed, rinsed with deionized water, and dried with nitrogen gas. A matrix of current magnitudes were tested during the experiment. Currents ranging from 10  $\mu\text{A}$  to 150  $\mu\text{A}$  were used. After several tests, the optimal electrodeposition conditions for achieving a polyaniline film with a thickness of 12 nm was determined. The deposition thicknesses were observed using spectroscopic ellipsometry. (J.A. Woollam V-VASE)



A stable deposition depended on many key conditions being met, such a clean platinum electrode, clean aniline solution, and a non-conductive back surface of the sample dipped in the aniline solution. Further explanation of the deposition parameters are included in the results and discussion section of this report.

### 2.2.3 Ellipsometric film characterization

Ellipsometry is an optical characterization technique based on sending polarized light into a sample and measuring the change in the phase of the light reflected from the sample to extract the optical properties and thicknesses of thin films[17]. The technique works best on sample surfaces which can reflect light. This makes ellipsometry better suited to measure a thinner film in contrast to an opaque film because an opaque film may absorb all of the incident light beam. The instrument can be used to measure the thickness, optical constants, surface roughness and uniformity of a sample and various other optical properties of materials[18]. In this project, ellipsometric data was gathered using a spectroscopic scan allowing the system to use varying wavelengths to measure the sample. In addition, the data was gathered from three different incident angles on the sample. With these parameters selected the instrument was able to estimate the properties of the electrodeposited material.

It is important to mention that although ellipsometry measures the optical properties of a sample, it relies on a library of predefined optical constant models to understand the deposited thin film. Electrodeposited polyaniline is not a commonly known material and does not have optical constants listed in the predefined library of the software. Therefore to extract the properties of this material, the literature suggested the use of the Cauchy equation to model this film. The Cauchy equation has been identified to properly model dielectrics and materials that are transparent in the visible region. The Cauchy-Urbach extinction dispersion equation was used to build a model to estimate the thickness of the polyaniline film. The results and analysis using this equation are found in the results and discussion section of this report.

#### 2.2.3.1 Thickness

The scalable test sample was mounted such that the incoming beam of the ellipsometer was centered in the middle of one of the circular openings of the sample. Thickness measurements were conducted in the high accuracy depolarized light mode. Spectroscopic scan was selected to run from 300 nm up to 1000 nm range in wavelength. The three angles of incident light on the sample surface were chosen to be 55°, 60°, and 65°.

### 2.2.3.2 Uniformity

Uniformity of the deposited film is an important parameter to help in the understanding of how the polyaniline film deposits on the surface of silicon. Uniformity measurements were desired at multiple points across the sample to get a complete understanding of surface variation. Ellipsometric uniformity measurements were therefore taken in a larger bare silicon surface to obtain multiple points in the measurement. The data of the variation of thickness across a sample is presented in the results and discussion section. Spectroscopic scan was selected to run from 300 nm up to 1000 nm range in wavelength. The three angles of incident light on the sample surface were chosen to be 55°, 60°, and 65°.

### 2.2.3.3 Repeatability

Repeatability of the measurement is an important parameter in verifying that the experiment can be done again from sample to sample. Of particular interest in this experiment was to figure out if the target thickness of 12 nm could be achieved for the same applied current and set time. Numerous repeatability test were done at different constant currents. Included in this report are four samples that were tested at the same current and end time with a target of 12 nm. Spectroscopic scan parameters and incident light angles stayed the same as uniformity and thickness test.

## **2.3 IMMOBILIZING ANTI ESCHERICHIA COLI ON POLYANILINE SURFACE**

Many techniques are used to immobilize biomolecules on a surface. The techniques commonly used include entrapment, covalent bonding, adsorption, microencapsulation, and affinity based techniques such as avidin-biotin interaction [19-21].

In this study, immobilization of the antibody was achieved through a series of steps that used avidin-biotin affinity complexation as well as covalent bonding. Covalent bonding was used to crosslink the avidin protein onto the polyaniline surface. Covalent bonding was also used to crosslink the biotin protein to the E. coli antibody through a process called biotinylation.

The two intermediate proteins (avidin and biotin) were linked together by taking advantage of the strong non covalent bond they form when reacted together. According to the literature, the avidin protein is known to have the ability to bind up to four biotin proteins due to its tetramer structure containing four identical subunits each for binding to biotin[21,

22] .The association constant of the bond these two proteins make with each other is reported as  $K_a = \sim 10^{15} M^{-1}$ [21, 23]. This bond has been reported as the strongest known affinity bond found in nature between ligand and protein[23].

Therefore with such a strong bonding affinity and specific attractive interaction between the two molecules, the biotin-avidin complex has received wide acceptance in strategies for immobilizing biomolecules[24]. The biotin-avidin complex is also known to be advantageous among other methods because it generally retains biomolecule activity more successfully[24].The system also represents a stable process for immobilization and has been found to be resistant to external stimulus such as pH, temperature, and denaturing solvents once the bond is formed[25]. This whole platform for immobilizing biomolecules onto conductive polymers via avidin-biotin complex is facilitated by using 3-diamine monohydrochloride (EDC) and N-hydroxysuccinimide (NHS) chemistries. These chemistries have been extensively used by numerous researchers to activate and crosslink protein to protein carboxyl groups with amine groups and improve protein immobilization in avidin-biotin complexation applications [10, 16, 26].

Due to the complexity of the immobilization chemistries in this report, the investigator focused on using spectroscopic studies to identity, verify, and characterize the presence of the protein used for each intermediate immobilization step in the procedure.

### 2.3.1 Experimental materials and methods

All biological experiments were carried out in the Biosafety 2 laboratory of Dr. Adrienne Minerick's Medical micro-Device Engineering Research Laboratory (M.D. - ERL) in chemical engineering. Fluorescence Microscopy studies were also conducted in M.D.- ERL. FTIR and Raman Spectroscopy studies were done in Dr. Yoke Kin Yap's research laboratory in the Department of Physics at MTU.

#### 2.3.1.1 Avidin immobilization on polyaniline surface

Crosslinking avidin with PANi followed a standard chemical procedure developed by Pierce, (a division of Thermo Fisher Scientific) that uses the chemicals 3-diamine monohydrochloride (EDC) and N-hydroxysuccinimide (NHS) to form a reactive solution. The chemical EDC is used to convert the carboxylic group of the avidin protein to make it amine reactive[25]. Once the amine reactive state is reached, the modified form is said to be unstable and will quickly hydrolyze[25]. NHS is incorporated in the solution to create a more stable amine reactive state[27]. At this point if the amine reactive avidin comes in contact

with the amine group of the polyaniline they will successfully crosslink and form a bond[25]. A pictorial description of the procedure for this device is shown below in figure 2.4.

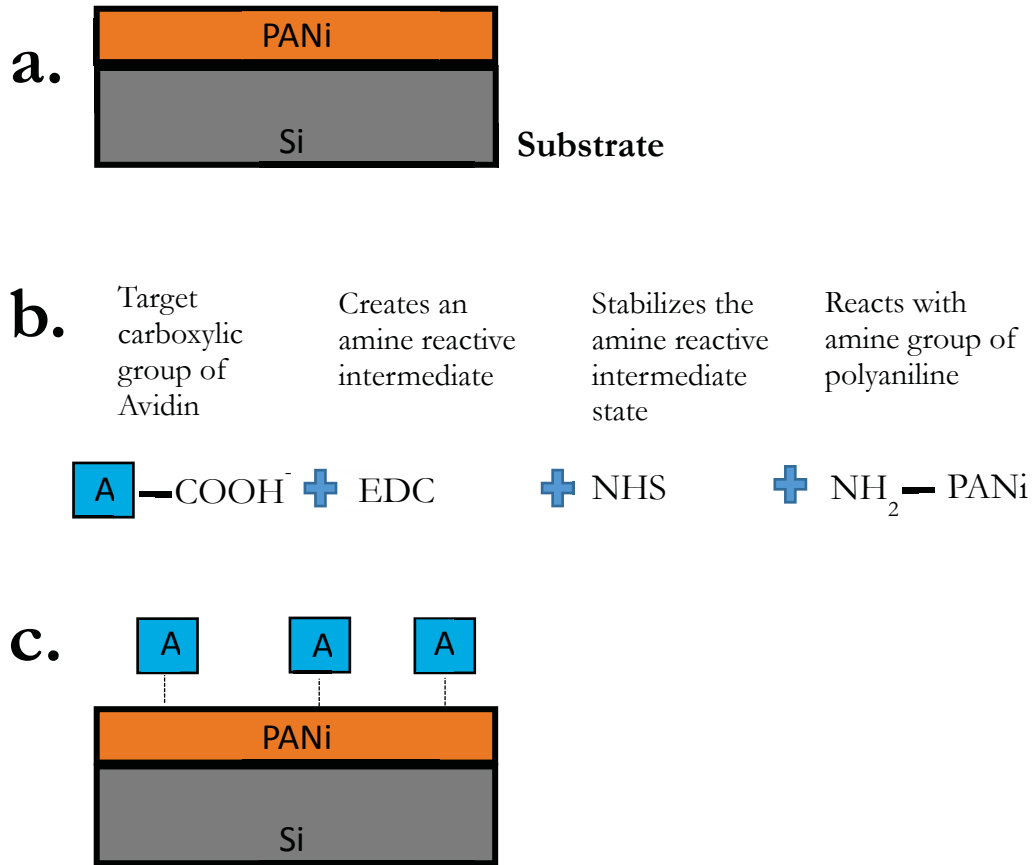


**Figure 2.4 Procedure for crosslinking avidin to PANi layer.**

- a. **Si substrate with PANi electrodeposited in circular region.**
- b. **The carboxylic group of avidin is reacted with EDC. The reaction creates an unstable intermediate amine reactive state. NHS is added to the solution to make the amine reactive intermediate state stable. The PANi layer is incubated with the avidin-EDC-NHS solution. The amine group of the PANi layer react with the amine reactive group of the avidin.**
- c. **The PANi layer crosslinks with the avidin protein.**

## Chemicals

Avidin, 3-diamine monohydrochloride (EDC) powder, N-hydroxysuccinimide (NHS) powder, Ultrapure water.

### Avidin activation and polyaniline crosslinking:

A solution containing Avidin protein (1 mg/1 ml) was prepared in ultrapure water. 0.3834 g of EDC (20 mM) was added to 0.4604 g of NHS (40 mM) in 1 ml ultrapure water. 10  $\mu$ L of the Avidin solution was added to the EDC/ NHS solution. The Avidin/EDC/NHS mixture was incubated for 30 min at room temperature. 10  $\mu$ L of Avidin/EDC/NHS was micropipette onto the PANi-Si substrates for 2 hours at room temperature. After the 2h incubation, the excess solution on the PANi-Si surface was rinsed with ultrapure water to flush unbound protein from the surface, and dried in a nitrogen gas stream.

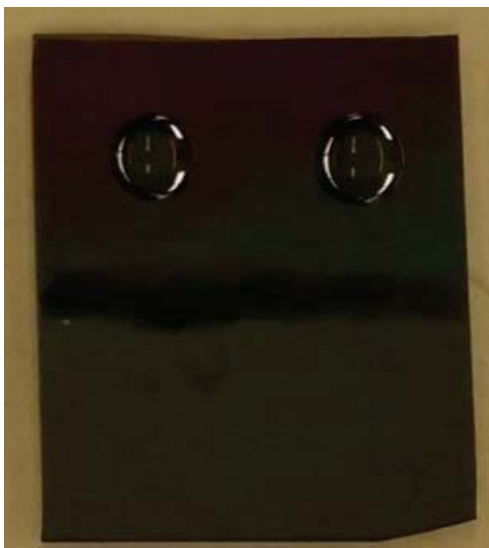


**Figure 2.5 PANi-silicon substrate incubation with 10  $\mu$ L Avidin/EDC/ NHS solution on surface.**

### 2.3.1.2 Anti-Escherichia coli O157:H7 Biotinylation Process

The antibody used in this study was E. coli O157 fluorescein isothiocyanate (FITC) conjugated purchased from Pierce. The antibody was purchased FITC conjugated (fluorescence tagged) for use in verifying the immobilization of the antibody on the polymer surface. All steps requiring handling and storage of the antibody were done in reduced lighting conditions in order to protect the fluorescence nature of the biomolecule.

The biotinylation procedure used in this experiment were followed according to EZ-Link Micro Sulfo-NHS-Biotinylation Kit instruction manual[28].

Crosslinking the biotin molecule with the antibody is known as biotinylation. The biotin used in this experiment was purchased as NHS-Biotin, which allowed the molecule to be amine reactive once measured in the solution. The amine reactive biotin was incubated with the antibody resulting in the crosslinking of the amine groups of the antibody and biotin. A pictorial description of the procedure for this device is shown below in figure 2.6.

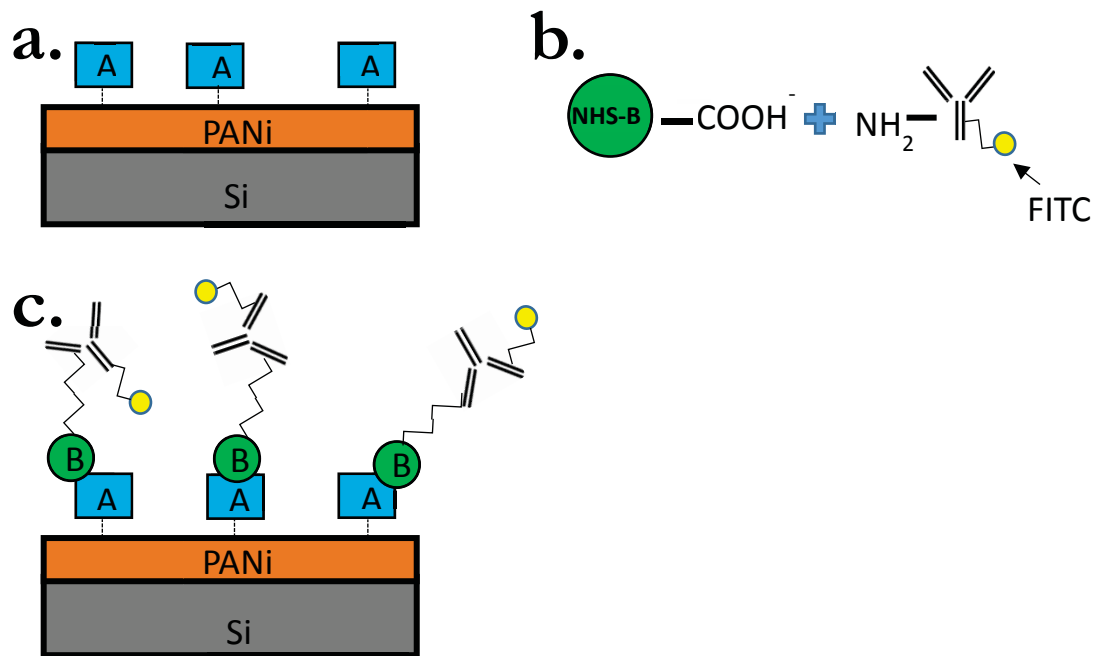


**Figure 2.6 Escherichia coli O157:H7 antibody immobilization sequence.**

- a. **Avidin protein is cross-linked with PANi layer.**
- b. **Carboxylic group of NHS-biotin is reacted with surface amine group of anti escherichia coli O157:H7 to achieve biotinylation.**
- c. **Incubation of biotinylated anti escherichia coli O157:H7 with PANi-avidin surface immobilizes anti escherichia coli onto substrate through avidin-biotin bonding.**

## Chemicals

Anti-Escherichia coli O157:H7 antibody, Pierce Kit (Sulfo-NHS Biotin), ultrapure water, Pierce Kit (Phosphate Buffered Saline), Zeba spin desalting columns.

### **Biotinylation Procedure:**

A microtube containing 200  $\mu\text{L}$  of purified Escherichia coli O157:H7 antibody was prepared. An amount of Sulfo-NHS biotin yielding a 50 molar excess of biotin to antibody was calculated for the reaction by following instructions from Pierce antibody kit shown in equations 1 & 2 below. 0.4  $\mu\text{L}$  of the Sulfo NHS Biotin was added to the 200  $\mu\text{L}$  of antibody solution. The solution was incubated in a microtube at room temperature for 1 hour. The unreacted biotin was removed from the solution through gel purification desalting columns using a Fisher Scientific Accuspin 400 centrifuge system. The Accuspin 400 centrifuge system was operated at 1000  $\times g$  for 2 minutes for each purification step.

Calculation to achieve a 50 molar excess of Sulfo-NHS Biotin.

1.

$$0.2 \text{ ml antibody} * \frac{.1 \text{ mg}}{1.5 \text{ mL}} * \frac{1 \text{ mmol IgG}}{150000 \text{ mg IgG}} * \frac{50 \text{ mmol Biotin}}{1 \text{ mmol IgG}} \text{ mmol} = 4.44 * 10^{-6} \text{ mmol Biotin}$$

2.

$$4.44 * 10^{-6} \text{ mmol Biotin} * \frac{443 \text{ mg}}{\text{mmol Biotin}} * \frac{200 \text{ uL DI water}}{1 \text{ mg}} = 0.393384 \text{ uL Biotin}$$

### 2.3.1.3 ANTI-ESCHERICHIA COLI O157:H7 IMMOBILIZATION:

Incubation of biotinylated anti E coli O157:H7 on Avidin/PANi/Si surface

The polymer substrate bound with avidin and the biotin conjugated antibody were gathered. 10  $\mu\text{L}$  of biotinylated antibody solution was micropipetted inside the Avidin/PANi/Si substrate 3.3mm diameter circles. 30  $\mu\text{L}$  of biotinylated antibody solution was micropipetted inside the Avidin/PANi/Si substrate 10 mm diameter circles. The reaction was incubated for 30 min at 25°C. After 30 min incubation the PANi coated substrates were rigorously rinsed in ultrapure water and nitrogen dried. The sensor was stored at -20°C when not in use.



## 3. Results and Discussion

### 3.1 CHALLENGES ENCOUNTERED DURING ELECTRODEPOSITION PROCESS

#### 3.1.1 Current density challenges

Electrodeposition measurements using the scalable test device was carried out by submerging the two circular silicon rings in the solution. Each ring is calculated to have an area of  $9.62 \text{ mm}^2$ . A total area of  $19.24 \text{ mm}^2$  was submerged in the aniline solution. Current density was then calculated as the amount of current applied to the working electrode divided by the total area submerged in the aniline solution.

Initially, step 6 of the fabrication process for the scalable test device was used a photoresist layer to cover the backside of the wafer. Experimental test with this design showed inconsistent film deposition thickness. Investigative studies showed the backside photoresist did not adhere to the unpolished side of the silicon wafer. Simple resistivity test on the backside of the wafer believed to have photoresist showed it was indeed conductive. With the backside of the wafer conductive the area of submerged substrate in the aniline solution varied from experiment to experiment. Therefore the current density changed in each experiment, leading to inaccuracies in repetitive polyaniline thickness studies. To solve this problem, a 50 nm sputtered silicon nitride film was deposited on the backside of the wafer. This adjustment proved successful in perfectly insulating the backside of the wafer, being unreactive to an activation hydrofluoric acid dip, and restricting the current density only to include the two circular silicon openings.

#### 3.1.2 Importance of clean electrodes

The platinum counter electrode may accumulate aniline residue on its surface after multiple experiments. This becomes a serious issues because aniline build up the electrode impedes the reaction speed. A normal deposition shows that as the film is growing in the exposed silicon regions, the potential rises because the resistance to the current flow is increasing with the increasing film thickness. With a contaminated platinum counter electrode, the rate of electrodeposition was slower and the Sourcemeter voltage rise was instable. The platinum electrode was submerged in an ultrasonic bath containing methanol for 10 minutes to completely clean the electrode of the polymer contamination.

### 3.1.3 Film saturation

Characterization of electrodeposited PANi films revealed there may be a point during the electrodeposition process where the film reaches saturation and will not continue to accumulate.

One conclusion to explain this behavior is as each successive layer of the PANi film stacks on the previous layer, it becomes increasingly more difficult to stack the film. In addition, depending on the amount of area exposed to the solution, a smaller area will reach saturation first. It is important to understand where this point is for the current density used. These parameters will help predict the largest consistent film thickness that can be grown within the controlled deposition area.

## 3.2 ELLIPSOMETRIC CHARACTERIZATION OF POLYANILINE

### 3.2.1 Modeling polyaniline films using Cauchy equation

Many films that are transparent in the visible light spectrum have optical parameters that can be modeled by the Cauchy equation[29]. The index of refraction of these types of films can be determined through ellipsometry by using the equation

$$n(\lambda) = A + \frac{B}{\lambda^2} + \frac{C}{\lambda^4} , \text{ [Equation 1]}$$

by specifying the constants A, B, and C in this equation. Using the experimental information generated by the ellipsometer it is possible to build a model that can be used to extract the film thickness[29].

An outline of how the Cauchy equation was used to extract information about electrodeposited polyaniline films will now be illustrated. After experimental ellipsometric spectroscopic data was acquired for a polyaniline sample, a graph of the index of refraction versus wavelength was observed. An example of this graph can be seen for an 80  $\mu\text{A}$  90 sec electrodeposition of a polyaniline film in figure 3.1 below.

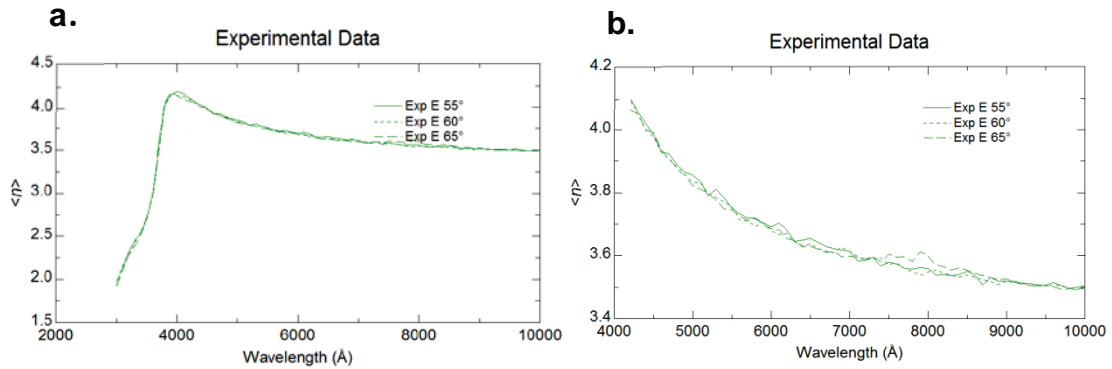


**Figure 3.1 Ellipsometric spectroscopic data for PANi film.**

- a. **Index of refraction versus wavelength spectrum for a 80  $\mu$ A 90 sec PANi electrodeposition.**
- b. **Index of refraction versus wavelength spectrum for 80  $\mu$ A 90 sec PANi electrodeposition excluding the high absorption region.**

From this graph it is observed that the film has the characteristic of absorbing light in the ultraviolet region seen by the large peak in that range (315 nm - 400 nm). This characteristic response cannot be described by using the Cauchy model because the peak included in the data is not accounted for by the simple Cauchy model[29]. This leaves the investigator with one of two choices to appropriately model this film. One option is to exclude a portion of the data that the Cauchy cannot accurately describe and bring it back in once information in the other region is understood[29].

In this example the investigator extracted a portion of the data in the region from 420 nm to 1000 nm and obtained the optical constants that accurately describe that region. (Figure 3.1 (b)) After extracting the optical constants at these higher wavelengths, regression analysis can be used to fit the data for the entire region including the peak.

### 3.2.2 Modeling polyaniline films using Cauchy-Urbach equation

The second option that can be used to characterize the polyaniline film is to use the Cauchy-Urbach equation model. This model is known to take into account the peak region in transparent films that absorb slightly in the ultraviolet region such as the observed experimental data generated for the polyaniline film shown in figure 3.1a[29].

The Cauchy- Urbach model uses the original Cauchy equation relating the index of refraction as a function of wavelength(Equation 1) with an equation relating the extinction coefficient as a function of wavelength (Equation 2) to generate the dispersion information for the material under study.

The Urbach equation relates the extinction coefficient as a function of wavelength for the material under study and is stated as follows

$$k(\lambda) = \alpha \exp \left\{ \beta \left[ 12400 \left( \frac{1}{\lambda} - \frac{1}{\gamma} \right) \right] \right\} \quad \text{[Equation 2]}$$

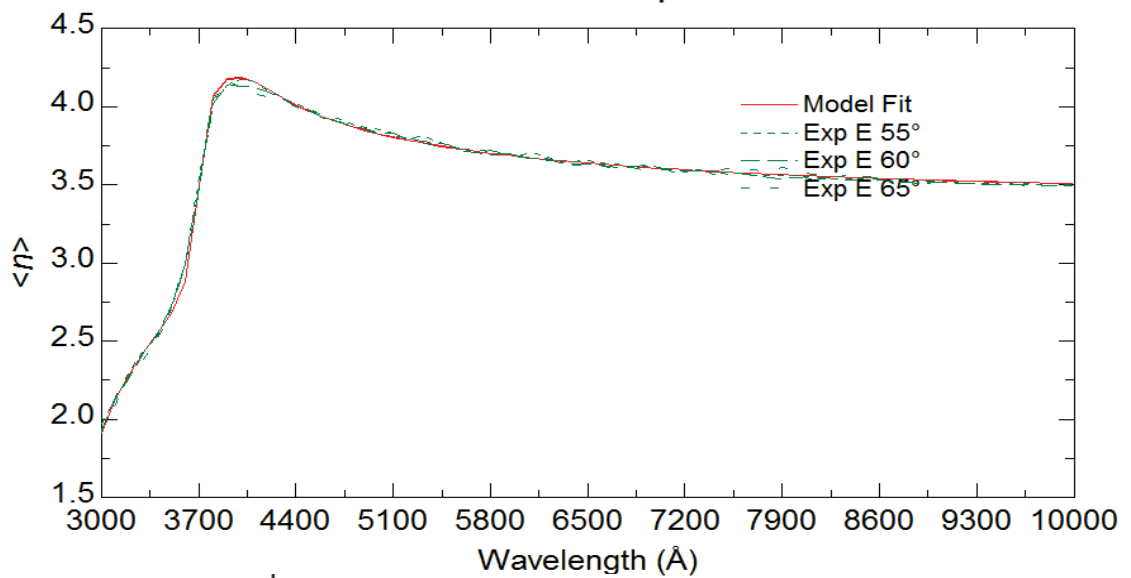
where  $\alpha$  is the amplitude term ,  $\beta$  is an exponential term,  $\gamma$  is the band edge[29, 30].

In this study, the amplitude parameter and the exponential parameter were chosen as fit parameters and the software used regression to determine their values. The band edge parameter was not used as a regression parameter in the analysis and was held fixed at the value of the lowest wavelength used[29, 30]. The lowest wavelength used for the study of these polyaniline films was 300 nm and therefore the band edge was chosen to be 300 nm.

For a typical measurement, a stack model was first created which contains the different layers of films deposited on the substrate. The stack model used for measuring the polyaniline film in this study is shown figure 3.2. The model is composed of a 0.5 mm silicon substrate as the base layer with a Cauchy layer representing the electrodeposited polyaniline stacked on top of it. After creating the film stack model, the band edge was the only parameter of the Cauchy-Urbach equation defined by the user. The band edge ( $\gamma$ ) was set to 300 nm. All of the other parameters were left to be fitted and regression analysis was performed by the J.A. Woollam software to determine the parameter values. The result of a measurement for a polyaniline film is shown in figure 3.2. The result shows the value of the film thickness calculated by the software as well as a good fit between the model and experimental data, the Cauchy-Urbach parameter values, and the calculated mean squared error. Ellipsometric analysis of polyaniline film thicknesses in subsequent chapters of this report are all based on the Cauchy - Urbach equation.

>	1 cauchy	10.024 nm
	0 silicon	0.5 mm

### Generated and Experimental



MSE	Final
Thick.1	10.024 ± 0.0521
An.1	1.9904 ± 0.0535
Bn.1	-0.079936 ± 0.0142
Cn.1	0.0041316 ± 0.000956
Ak.1	0.056624 ± 0.00663
Bk.1	0.16059 ± 0.117

**Figure 3.2 Ellipsometric analysis of a PANi film thickness based on the Cauchy- Urbach equation. The figure shows an excellent match was achieved with the modeling equation used to fit the experimental data and a low MSE value was obtained.**

### 3.2.3 Thickness results

The results of final polyaniline film thickness versus current density are shown below. Each experimental test was carried out by applying 5 different source constant currents to the working electrode. The deposition time was fixed at 90 sec for each run. An increase in current density shows that there will be an increase in the deposition rate of the film.

**Table 3.1-**The effect of current density on the growth rate of PANi film.

Applied current ( $\mu\text{A}$ )	Deposition time (sec)	Current density ( $\mu\text{A}/\text{cm}^2$ )	Film thickness (nm)	Effective deposition rate(pm/sec)
10	90	51.97	3.735	41.5
30	90	155.93	6.178	68.6
50	90	259.88	7.740	86.0
80	90	415.80	10.024	111.4
100	90	519.75	11.423	127

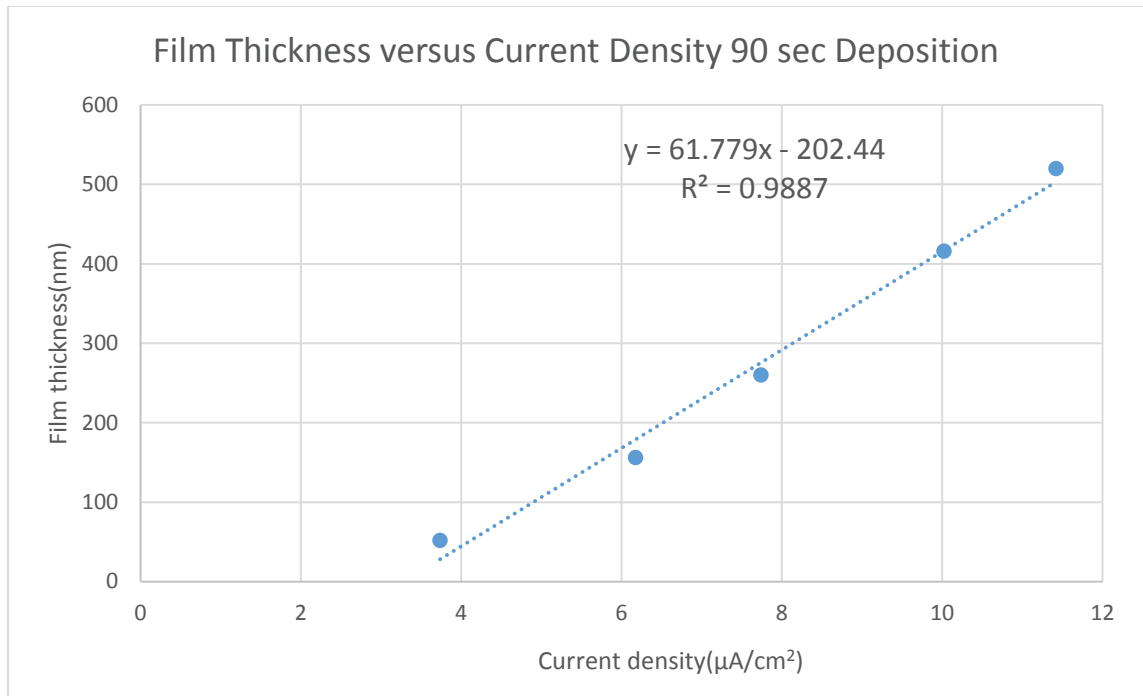


**Figure 3.3 Film thickness versus current density for 5 PANi samples.**

#### 3.2.4 Uniformity results

The results of an electro deposition experiment with an applied current of 80 μA and 60 sec deposition time is shown below. A 141 mm<sup>2</sup> piece of bare silicon substrate was submerged in the polyaniline solution for this experiment. Twenty thickness values were measured across the sample surface using spectroscopic ellipsometry to gather the data. Film thickness values center around the mean value of 8.875 nm. The standard deviation was calculated to be 0.854. It was observed that film thickness had a tendency to be thicker at the edge of the sample. The thickness of the film in the center of the sample varied less over distance.

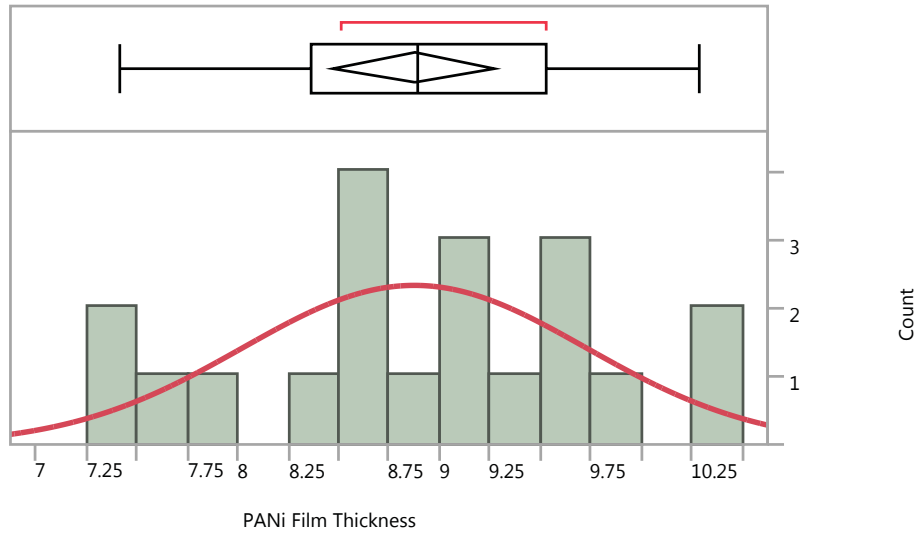


**Figure 3.4 Variation of PANi film thickness across sample**

Normal(8.8758,0.85361)

**Table 3.2-** Uniformity distribution of an electrodeposited PANi film.

**Summary Statistics**

Mean 8.8758  
 Std Dev 0.8536101  
 N 20  
 Minimum 7.411  
 Maximum 10.291

**Fitted Normal**

**Parameter Estimates**

Type	Parameter	Estimate	Lower 95%	Upper 95%
Location	$\mu$	8.8758	8.4762982	9.2753018
Dispersion	$\sigma$	0.8536101	0.6491623	1.2467587

$-2\log(\text{Likelihood}) = 49.4263105109622$



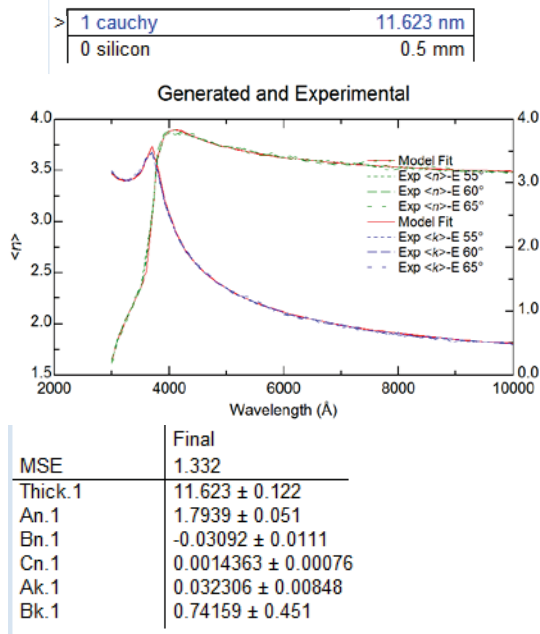
### 3.2.5 Repeatability results

Electrodeposition experiments were conducted to test the repeatability of achieving the same film thickness using 4 different samples. Experimentation was carried out to reach a target film thickness of 12 nm. The depositions were carried out with an applied current of 100  $\mu\text{A}$  for 90 sec. Results for the 4 samples are shown in table 3.3 & figure 3.5 below. The film thickness of figure (c) sample and figure (d) sample were slightly thicker than figure (a) sample and figure (b) sample. The ellipsometric data analysis shows that the model and experimental data for figure (c) sample and figure (d) sample tend to deviate from the Cauchy fit providing a reason why the films thicknesses were slightly different. Also, perhaps the slight change in the experimental data occurred because the electrodeposition of films (c) and (d) were done on a separate day than films (a) and film (b).

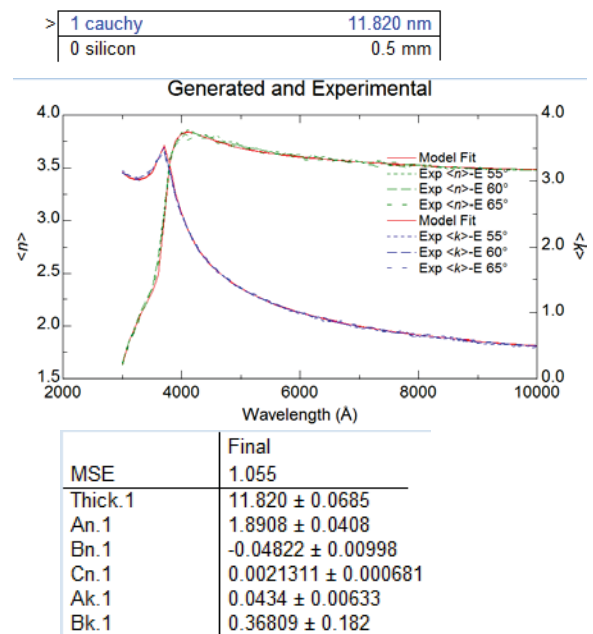
**Table 3.3-** Test of the repeatability of PANi deposition

Applied current ( $\mu\text{A}$ )	Deposition time (sec)	Current density ( $\mu\text{A}/\text{cm}^2$ )	Film thickness (nm)
100	90	519.75	11.623
100	90	519.75	11.820
100	90	519.75	12.713
100	90	519.75	12.096
Average Thickness (nm) = 12.063		Standard Deviation in Thickness (nm) = 0.4112	

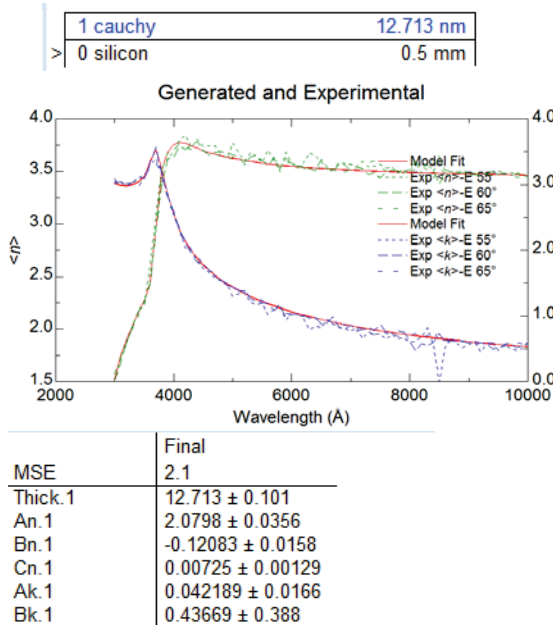
a. Sample 1.



b. Sample 2.



c. Sample 3



d. Sample 4

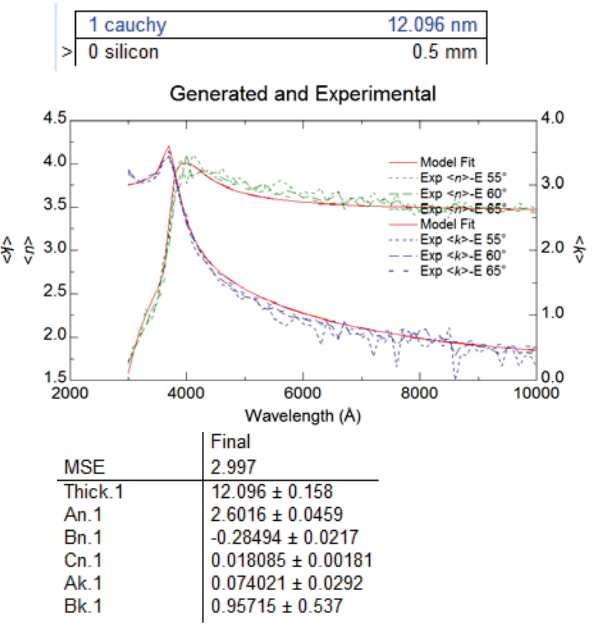


**Figure 3.5 (a,b,c,d) Test of electrodeposition process to repeatedly create a 12 nm PANi film.**

### 3.2.6 Ellipsometric challenges with large angle measurements

Large angle measurements using the ellipsometer were inaccurate for the samples used in this experiment. The spot size of the ellipsometer beam was more than half the size of the 3.5 mm diameter sample area. When probing the sample surface at angles of incidence greater than  $70^\circ$  the reflected light may have returned through adjacent layers of the substrate. This caused the data to be composed of information including polyaniline, silicon oxide, and photoresist. The measurement was adjusted to use smaller angles between  $55^\circ$  to  $65^\circ$  and successful thickness measurements were received.

## 3.3 IMMOBILIZING ANTI ESCHERICHIA COLI ON POLYANILINE SURFACE RESULTS

### 3.3.1 Verifying avidin protein crosslinking with polyaniline

A stepwise approach was used to evaluate the effectiveness of each immobilization step in hopes of identifying and modifying problems in activation chemistries. Verifying the binding of the avidin protein to the surface of the polymer was the first task and the results from that study are explained in the following discussion.

#### 3.3.1.1 Ellipsometric surface thickness change results

The ellipsometer is sensitive enough to detect small changes in the thickness of a thin film. The instrument was used in this study to make a comparison between the change in thickness of the substrate-polymer surface before and after the avidin binding procedure. The results of this study are shown in table 3.4.

There is a clear agreement between the 6 samples that the thickness of polymer surface has changed and thus it can be concluded binding has occurred. Figure 3.6 shows a graphical representation of the surface thickness changes. Overall, the six sample measurements show the change in the polymer surface thickness is consistent between each sample with a mean value of 4.8 nm. Two monomers of the avidin protein were experimentally shown to have a crystal spacing of  $a = 72.22 \text{ \AA}$ ,  $b = 80.42 \text{ \AA}$ ,  $c = 43.33 \text{ \AA}$  [31]. Ellipsometric data collected in this study show a close relationship between the experimental value of the length obtained for the avidin protein (4.8nm) to the protein crystal study done on avidin showing an average length between 4 – 8 nm for the protein[31].

**Table 3.4-** Ellipsometric avidin protein binding results:

Sample set	Measured thickness before avidin binding	Film thickness after avidin binding	Statistics
Sample 1	12.44 nm	17.44 nm	Mean difference = 4.797 nm Maximum = 6.1 nm Minimum = 3.73 nm STD = 0.8811 nm
Sample 2	19.5 nm	24.876 nm	
Sample 3	9 nm	13.97 nm	
Sample 4	9.19 nm	12.8 nm	
Sample 5	12.973 nm	16.7 nm	
Sample 6	17.9 nm	24 nm	

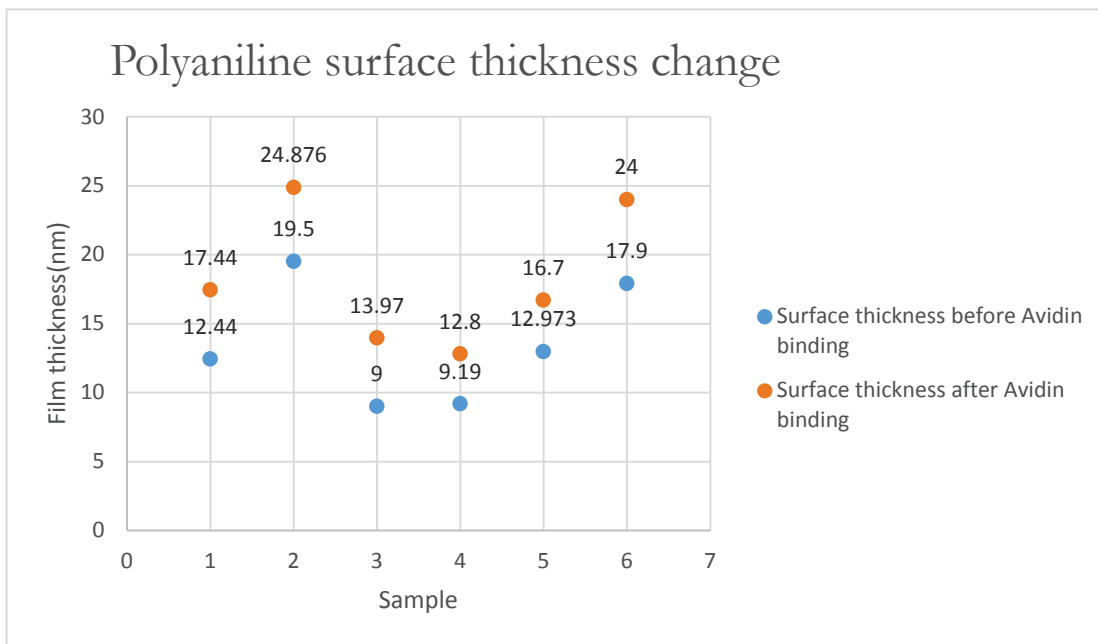


**Figure 3.6 Change in PANi surface thickness due to avidin binding. A consistent change in thickness is observed over a range of starting thicknesses.**

### 3.3.1.2 Fourier transform infrared spectroscopy results

The method of Fourier Transform Infrared spectroscopy (FTIR) was sought because A. Deep, et al. [16] used FTIR to prove the immobilization of anti-human IgG on PANi films. Their study made a comparison of the FTIR spectra before and after antibodies were immobilized on a PANi surface and they were able to document the presence of the antibodies by identifying new characteristic peaks in the FTIR spectra. Following this same logic, we performed an investigation of whether the presence of the avidin protein on the PANi coated substrate could be detected.

The instrument used for the study was a Jasco Fourier Transformed Infrared Spectrometer operated in the spectral range of  $350\text{ cm}^{-1}$  to  $4000\text{ cm}^{-1}$ . To keep measurement consistent, the 5 samples used in the ellipsometric measurement were investigated with the FTIR instrument. Preparations were made such that the sample spectrums were first measured with the ellipsometer, followed by a measurement with FTIR. After the avidin binding procedure was completed the same measurement procedure was followed.

FTIR was used to measure samples in the transmission mode. Results from one of the FTIR measurements are shown in figure 14. As observed, the FTIR spectrum for the sample presented no significant peaks to characterize the PANi film. Close observation of the amount of signal transmitted through the sample (shown on the y-axis), revealed that all the radiation was transmitted through the sample over the entire spectral range. The sample showed no significant sign of absorbing infrared radiation. Measurement of all other samples showed the same characteristics. Therefore the use of FTIR was inconclusive in investigating the binding of avidin to the polyaniline film.

One possible reason why the measurement did not produce a spectral characteristic for the polymer film may be because the instrument normally measures materials deposited on a lightly doped Si substrate. The Si substrates used in this experiment were heavily doped in order to enhance the electrodeposition process. The response of the instrument to PANi on heavily doped Si were therefore different than expected for infrared radiation through a heavily doped substrate.

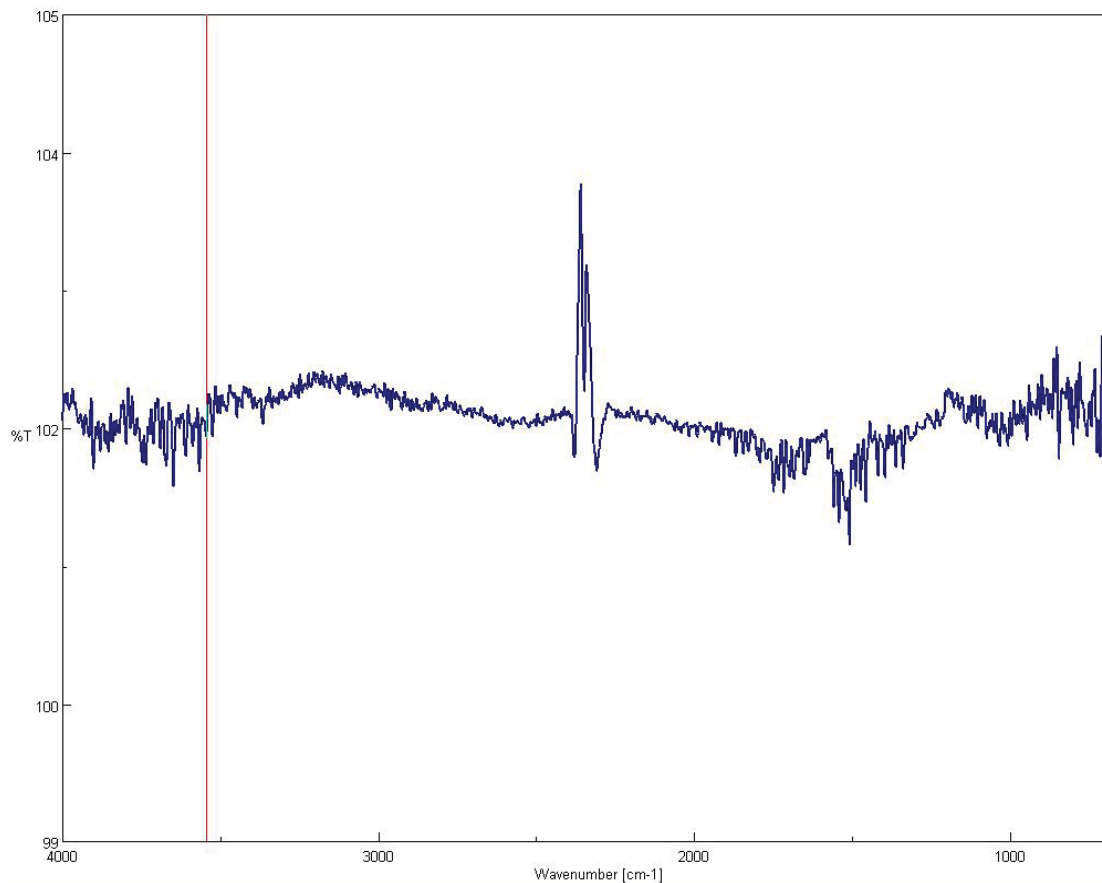


***Figure 3.7 FTIR transmission spectrum measured for PANi on heavily doped Si. Results show a signal was generated centered around 102%. The peaks in the spectrum are meaningless because the 100% transmission is the best a sample can transmit. This information could not be explained and provided no information about the sample properties.***

### 3.3.2 Verifying antibody immobilization with polyaniline

#### 3.3.2.1 Raman spectroscopy results

Raman spectroscopy was used to identify the structural properties of the polyaniline films. The instrument used for the study was a Jobin-Yvon LabRAM HR800 Raman Spectrometer operated with an excitation wavelength of 633 nm.

#### **Investigation before antibody immobilization:**

In the first experiment shown in figure 3.8, three silicon substrates were coated with different thicknesses of PANi and studied. Testing of all films showed a characteristic peak centered around  $520\text{ cm}^{-1}$  representing the silicon substrate.(not shown)

The Raman spectrum shown in gray and orange in figure 3.9 are the result of an 11 nm and 18 nm PANi film electrodeposited on Si. The Raman spectrum revealed one peak response around  $940\text{ cm}^{-1}$ . Although this peak represented a spectral response, it does not provide any identifying characteristics of the polyaniline film found in literature. However, the Raman spectrum for the 50 nm PANi film shows two prominent peaks indicative of a polyaniline film. The peaks around  $1193\text{ cm}^{-1}$  and  $1623\text{ cm}^{-1}$  in the Raman spectrum of polyaniline are indicative of its structure which is composed of repeated benzene rings[32, 33].

Based on the results of the 50 nm film, 3 new PANi samples were made to access the repeatability of the thick film Raman result. After collecting data from the 3 thick films, a comparison of their Raman spectra showed a spectrum closely related to what is found in literature Raman studies of polyaniline films. An investigation of polyaniline films by Arsov et al. showed 5 Raman spectrums, each representing a different voltage applied to the working electrode. The similarities of Arsov et al. study with our experimental data are evident in the Raman peaks around  $1193\text{ cm}^{-1}$  and  $1623\text{ cm}^{-1}$ . The other peaks found in between the two prominent peaks in the spectra were also found in my results. The other peaks were explained as signals that represent the degree of oxidation the PANi film experienced from the electrodeposition process[32].

### **Investigation after antibody immobilization:**

The method of identifying the immobilization of proteins in a PANi substrate has been demonstrated by Deep et al. In their study the researchers were able to show the emergence of two additional peaks in the Raman spectra after the immobilization of anti-human IgG to a PANi coated surface[16].

Based on this proven method, Raman was used to investigate the immobilization of e coli antibodies on the surface of PANi. Raman studies of the polyaniline surface after antibody immobilization were unsuccessful in providing evidence of any antibody immobilized on the polymer surface. 3 samples were tested and multiple scans of their surfaces were acquired. The results showed a consistent response corresponding to the structure of polyaniline. However no new peaks or shifting of peaks in the Raman spectrum were detected to confirm the presence of e coli antibody.

It is my conclusion that Raman spectroscopy was unsuccessful in identifying the E. coli antibodies immobilized on the PANi surface because the density of the antibody distributed across the polymer surface was very low. (The weak signal from fluorescence imaging later confirmed this hypothesis.) Therefore it was concluded that the Raman spectroscopy was looking for a very small signal among a large amount of polymer.



### Raman Spectroscopy of PANi films

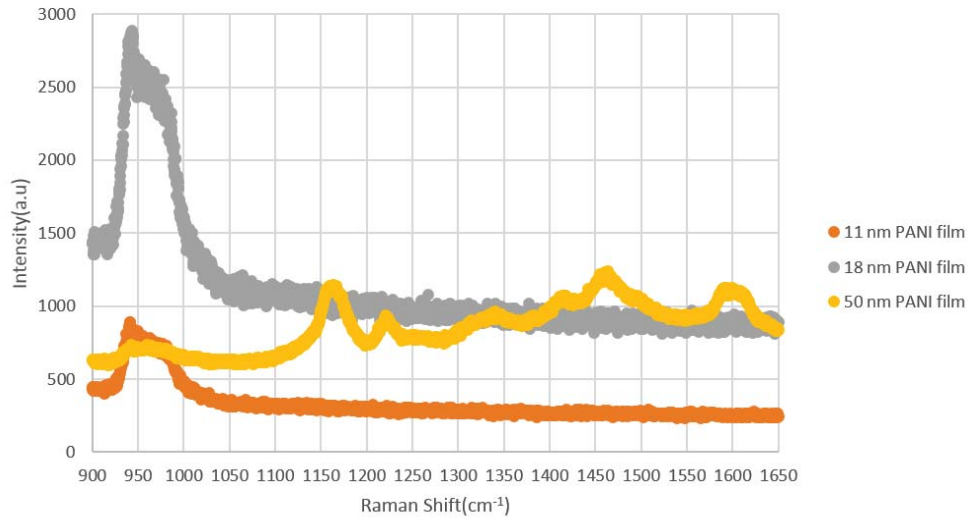


**Figure 3.8 Raman spectrum of 3 PANi films of different thicknesses. Study revealed films greater than 50 nm produced characteristic peaks of PANi and were better detected with Raman spectroscopy.**

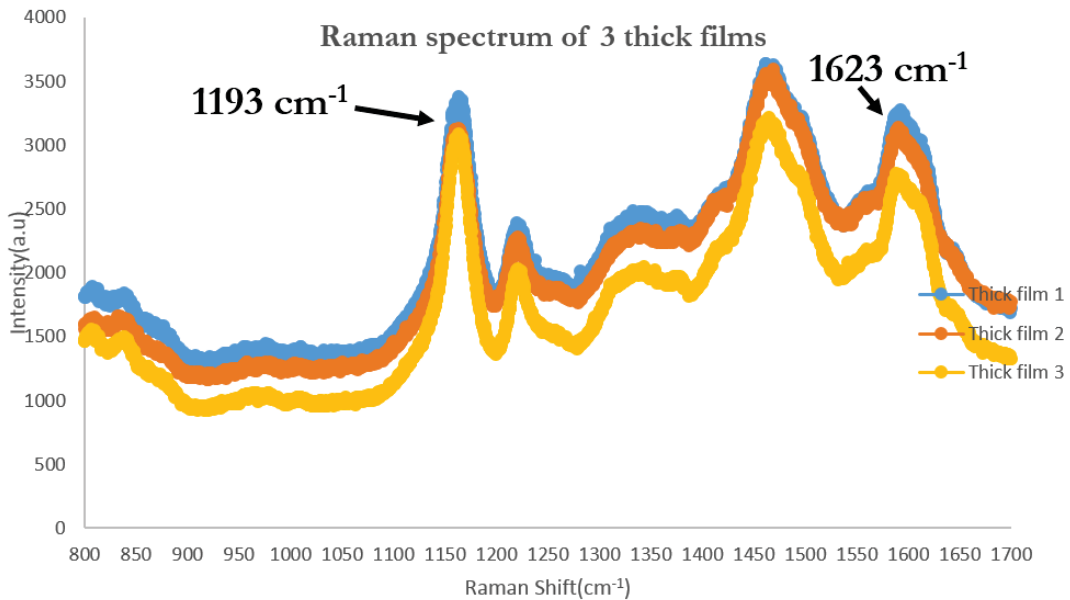


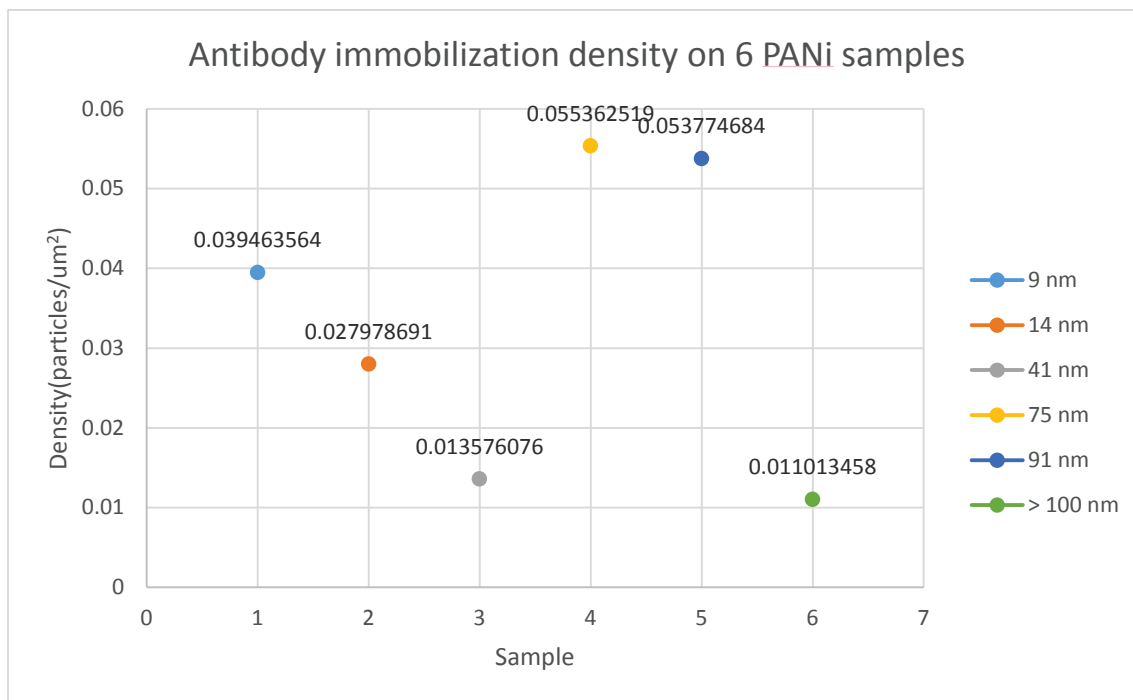
**Figure 3.9 Raman spectroscopy of 3 thick PANi films to determine the repeatability of characteristics Raman peaks.**

### 3.3.3 FLUORESCENCE MICROSCOPY RESULTS

Significant results were acquired from fluorescence microscopy to prove FITC conjugated antibodies were immobilized on the PANi surface. Figure 3.12 displays the fluorescence image results for the samples used in this study. Image J software package was used to count the number of particles in each image and to determine the area of the image in order to determine the density of particles in each image. It was observed that an average of 0.033528 antibody per  $\mu\text{m}^2$  were incorporated in each of the samples used. Figure 3.10. displays the density of immobilized antibodies measured for each sample. Although the results proved antibodies were immobilized on the PANi surface, it also revealed the antibody density on the PANi surface was small. This understanding gave explanation why previous Raman spectroscopy studies of the PANi surface in search for immobilized antibody were unsuccessful.

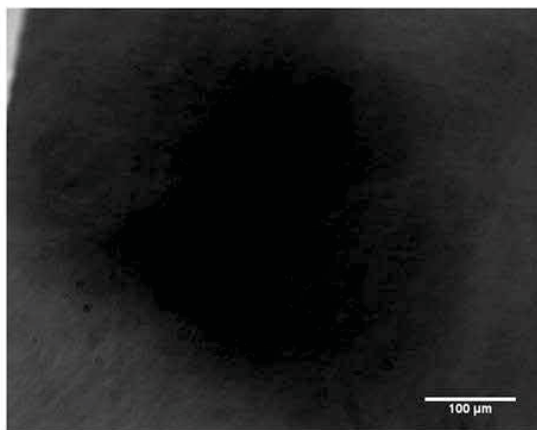
In addition, the results showed that PANi films surfaces as thin as 9 nm and 14 nm were able to be modified to incorporate the antibodies. (Figure 3.12a - 3.12b). This is significant because the results prove that we have a method to create very thin PANi films with antibodies immobilized on them that can be used in forming a bio-electrode for a biosensor. This thin sensor coatings can possibly contribute to better sensitivity of the device.

Figure 3.12c and 3.12d are the results obtained for very thick PANi films on Si. The images show the non-uniform nature of thicker films as they tend to have discontinuities in their film layers due to the large stress due to growth during the electrodeposition process. It is interesting to point out that the areas in the thick films where the underlying silicon layer is revealed show clean bare silicon surfaces. This can be one way of evaluating that the antibodies immobilized on the polymer are indeed due to avidin-biotin binding and not from improper cleaning of the surface. Figures 3.11a and 3.11b show the control sample for this experiment. The control experiment in figure 3.11a reveals a clean PANi surface layer before any surface modification. The image in figure 3.11b shows the control consisting of a PANi substrate with 30 $\mu\text{L}$  of antibody on its surface without EDC and NHS modification. The measured antibody density on this control surface was 0.015533935 particles/ $\mu\text{m}^2$ .



**Figure 3.10** The density of immobilized antibodies measured for 6 PANi samples with different film thicknesses.

a.



b.

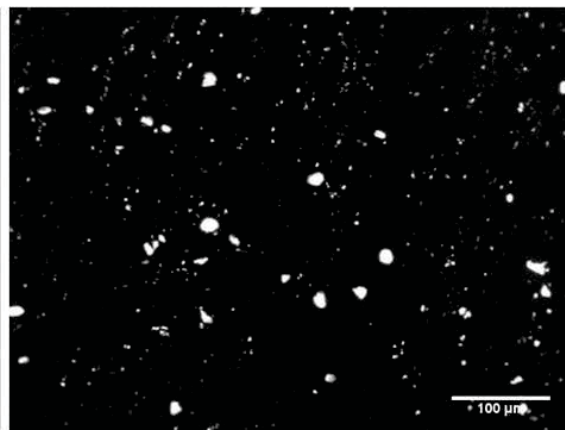


**Figure 3.11** Fluorescence images of control samples.

(a) Control sample showing PANi coated surface without antibodies  
 (b) Control sample showing 30 μL of antibody on surface (before immobilization chemistries)

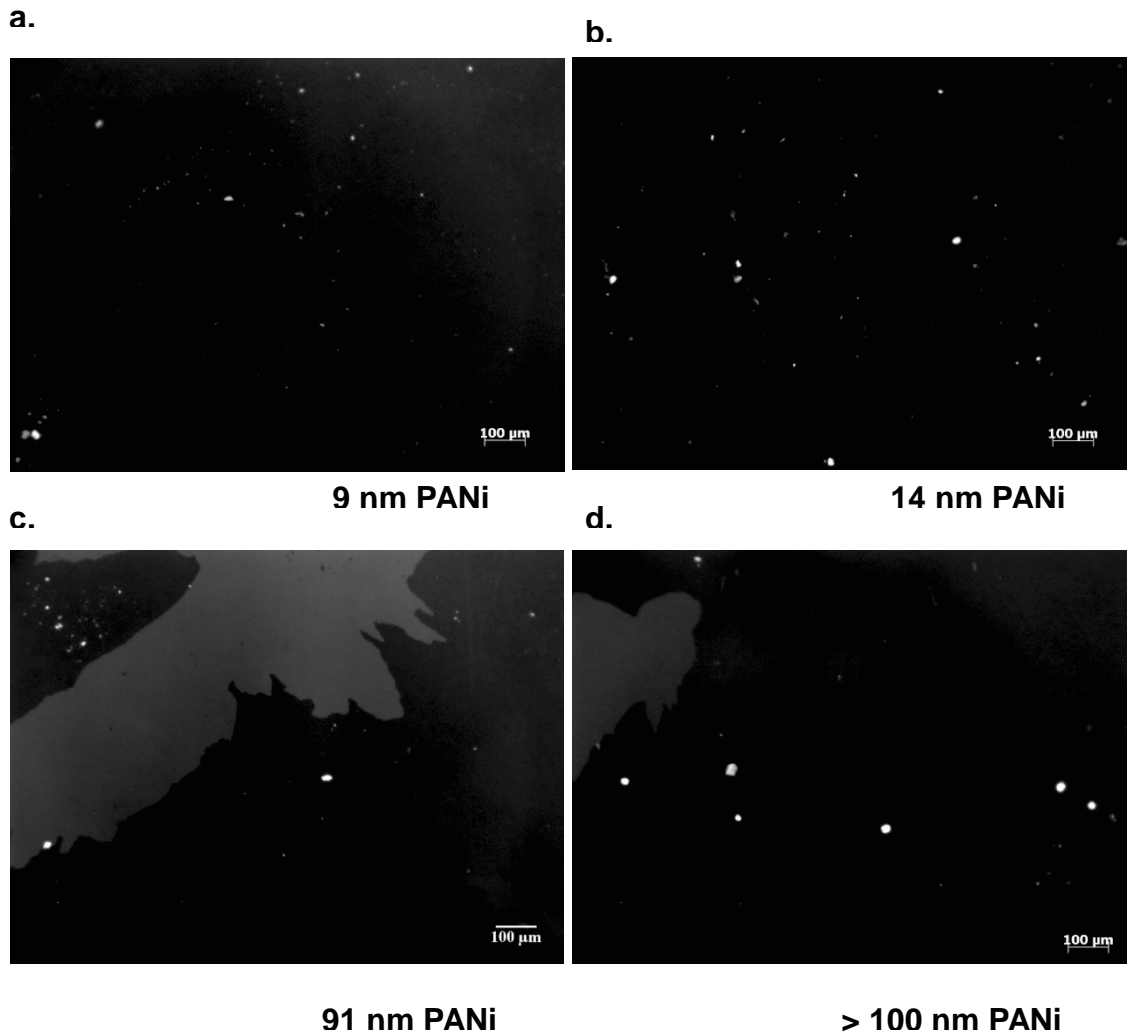


**Figure 3.11** Fluorescence images of immobilized *e. coli* antibodies on 4 different PANi substrates. All PANi samples displayed a moderate amount of antibody immobilization density and film thicknesses as low as 9 nm could be immobilized with antibodies.

## 4. CONCLUSION

The experiment proved polyaniline thin films could be electrodeposited on silicon in a reasonably uniform and repeatable manner. Ellipsometric investigation of the polyaniline layer proved sensitive enough to characterize the thickness of the films and in investigating changes in the film thickness from intermediate avidin protein binding. Raman spectroscopy assisted in identifying of the form of the polymer and in characterizing its conductive state. Fluorescence microscopy verified the immobilization of e coli antibodies to the surface of polymer through the method of avidin biotin interaction. Although the density of antibodies immobilized on the polymer surface were not as desired, the results provide an idea of what adjustments to the chemistries may possibly lead to increased antibody immobilization.

## 5. FUTURE WORK

### 5.1 Electrodeposit using cyclic voltammetry method

In this study, the constant current source approach was applied to grow PANi films on Si substrates. The method was convenient and simple to use, requiring only a current source and the ability to also detect the voltage. Although the current source approach produced good quality films, the method had drawbacks because it did not provide any information during and after the deposition process about the characteristics of the film.

Consideration of electrodepositing PANi films using cyclic voltammetry in conjunction with a program that provides graphical analysis of the current applied versus voltage measured during the deposition process should be thought about for future work. Unlike the constant current approach, cyclic voltammetry provides a much better way to analyze PANi films as revealed from a large percentage of the literature based on PANi film growth using cyclic voltammetry. Cyclic voltammograms produced from cyclic voltammetry provide information such as redox peaks representing the time during the electrodeposition process. They also provide information on when the film transitions from its insulating form to conductive form. Information to better gauge what current density to use and resulting film thickness can also be estimated from the cyclic voltammograms. Therefore future work should take this method into consideration due to the amount of information that can be gained.

### 5.2 Optimize process to increase antibody density

Since this technology is intended to be used to create a biosensor, the amount of antibody immobilized on the PANi is critical to the overall sensitivity of the device. Fluorescence imaging results revealed the density of the antibody immobilized to the PANi were very low.

During fluorescence microscopy, the investigator noticed the corners of the samples were covered with a significant amount of antibody. This makes sense because the sample was rinsed with ultrapure water, with the stream of the rinse water flowing towards the edge of the sample. However, this result showed that much of the antibodies which were not bound to the surface did not successfully conjugate with biotin protein. This is an indication that the biotin protein either did not bind to the avidin or did not bind to the antibody. Logically, it would make sense that the biotin did not bind with enough antibodies and therefore causing unbound antibodies to be rinsed off the sample during cleaning. The investigator suggests future experiments focus on increasing the concentration and incubation time of biotin used in the experiment to increase antibody incorporation.

### 5.3 Reduce avidin concentration

The investigator would like to suggest a future study which explores the use of the avidin molecule in a lower concentration. The avidin layer formed on the polyaniline surface in this study was crosslinked with the polymer using a high concentration. It has been demonstrated that excess free avidin molecules can lead to a competition between the bound avidin molecules for the attachment of antibodies[34]. Therefore if there was indeed free avidin molecules not bound to the polyaniline surface, this may have contributed to reason why the results obtained in this study showed low antibody density.

### 5.4 Investigate avidin biotin complex only

An alternative measurement that is worth understanding is the binding of avidin and biotin(without antibodies) bound on the polyaniline surface. Ellipsometric characterization and modeling details can be used once again to measure changes in surface thickness. There is much literature on the avidin biotin complex that can provide information on how large the molecules are together and characterization of this configuration[31]. This measurement may also be helpful in the understanding of which step of the chemistries lead to the low antibody density in this study.

## 6. References

1. Centers for Disease Control and Prevention. *General informaton Escherichia coli(E. Coli)*. 2012 August 3, 2012 December 4, 2014]; Available from: <http://www.cdc.gov/ecoli/general/index.html>.
2. Centers for Disease Control and Prevention. *Reports of Selected E. coli Outbreak Investigations*. 2014 May 22, 2014 December 4, 2014]; Available from: <http://www.cdc.gov/ecoli/outbreaks.html>.
3. Muhammad-Tahir, Z. and E.C. Alocilja, *Fabrication of a Disposable Biosensor for Escherichia coli O157:H7 Detection*. IEEE 2003. **3**(4): p. 345-351.
4. Gould, L.H., et al., *Update: Recommendations for Diagnosis of Shiga Toxin-Producing Escherichia coli Infections by Clinical Laboratories*. Clinical Microbiology Newsletter, 2012. **34**(10): p. 75-83.
5. Ake, J.A., et al., *Relative Nephroprotection During Escherichia coli O157:H7 Infections: Association With Intravenous Volume Expansion*. PEDIATRICS, 2005. **115**(6): p. e673-e680.
6. Settingington, E.B. and E.C. Alocilja, *Electrochemical Biosensor for Rapid and Sensitive Detection of Magnetically Extracted Bacterial Pathogens*. Biosensors, 2012. **2**: p. 15-31.
7. Food and Drug Administration, *Bad Bug Book, Foodborne Pathogenic Microorganisms and Natural Toxins*. 2 ed. 2012.
8. Berkenpas, E., P. Millard, and M. Pereira da Cunha, *Detection of Escherichia coli O157:H7 with langasite pure shear horizontal surface acoustic wave sensors*. Biosensors & Bioelectronics, 2006. **21**: p. 2255-2262.
9. Mulchandani, A. and N.V. Myung, *Conducting polymer nanowires-based label-free biosensors*. Curr Opin Biotechnol, 2011. **22**(4): p. 502-8.
10. Arora, K., et al., *Escherichia coli Genosensor Based on Polyaniline.pdf*. Analytical Chemistry, 2007. **79**(16): p. 6152-6158.
11. Penner, R.M., *Chemical sensing with nanowires*. Annu Rev Anal Chem (Palo Alto Calif), 2012. **5**: p. 461-85.
12. Li, Z., et al., *Sequence-Specific Label-Free DNA Sensors Based on Silicon Nanowires*. American Chemical Society, 2004. **4**(2): p. 245-247.
13. Arshak, K., et al., *Conducting polymers and Their Applications to Biosensors: Emphasizing on Foodborne Pathogen Detection.pdf*. IEEE, 2009. **9**(12): p. 1942-1951.

14. Poet, D.T.D., et al., *Direct electron transfer with glucose oxidase immobilized in an electropolymerized poly (N-methylpyrrole) film on a gold microelectrode*. *Analytica Chimica Acta*, 1990. **235**: p. 255-263.
15. Rajesh, T. Ahuja, and D. Kumar, *Recent progress in the development of nano-structured conducting polymers/nanocomposites for sensor applications*. *Sensors and Actuators B: Chemical*, 2009. **136**(1): p. 275-286.
16. Deep, A., et al., *Nanostructured polyaniline–silicon substrate for protein biosensing*. *Sensors and Actuators B: Chemical*, 2012. **171-172**: p. 210-215.
17. Fujiwara, H., *Spectroscopic ellipsometry: Principles and applications*. 2007, Chichester, England: John Wiley & Sons.
18. J. A. Woollam Co. Inc, *Guide to Using WVASE Spectroscopic Ellipsometry Data Acquisition and Analysis Software*. 1994: J.A Woollam Co.
19. Eggins, B.R., *Chemical Sensors and Biosensors( Analytical Techniques in the Sciences(ANTSS))*. 2002, England: John Wiley & Sons. 300.
20. Malhotra, B.D., A. Chaubey, and S.P. Singh, *Prospects of conducting polymers in biosensors*. *Anal Chim Acta*, 2006. **578**(1): p. 59-74.
21. Anzai, J.I., T. Hoshi, and T. Osa, *Avidin-biotin complexation for enzyme sensor application*. *Trends in Analytical Chemistry*, 1994. **13**(5): p. 205-210.
22. Wilchek, M., E.A. Bayer, and O. Livnah, *Essentials of biorecognition: the (strept)avidin-biotin system as a model for protein-protein and protein-ligand interaction*. *Immunol Lett*, 2006. **103**(1): p. 27-32.
23. Livnah, O., et al., *Three-dimensional structures of avidin and the avidin-biotin complex.pdf*. *Biochemistry*, 1993. **90**: p. 5076-5080.
24. Cosnier, S., *Biosensors based on electropolymerized films: new trends*. *Anal Bioanal Chem*, 2003. **377**: p. 507-520.
25. Hayworth, D. *Carbodiimide Crosslinker Chemistry*. 2014 December 4, 2014]; Available from: <http://www.piercenet.com/method/carbodiimide-crosslinker-chemistry#carbodiimide>.
26. Tully, E., S.P. Higson, and R.O. Kennedy, *The development of a labelless immunosensor for the detection of Listeria monocytogenes cell surface protein, Internalin B*. *Biosensors and Bioelectronics*, 2008. **23**: p. 906-912.
27. Hayworth, D. *Chemistry of Crosslinking*. 2014 [cited 2014 December 4, 2014]; Available from: <http://www.piercenet.com/method/chemistry-crosslinking>.
28. Thermo Fisher Scientific. *EZ -Link-Sulfo-NHS-SS-Biotin*. 2012 [cited 2015 February 28, 2015]; Available from: [https://tools.lifetechnologies.com/content/sfs/manuals/MAN0011183\\_EZ\\_Sulfo\\_NHS\\_SS\\_Biotin\\_UG.pdf](https://tools.lifetechnologies.com/content/sfs/manuals/MAN0011183_EZ_Sulfo_NHS_SS_Biotin_UG.pdf).



29. Tompkins, H.G., in *WVASE32 Software Training Manual* 2006, J.A. Woollam Co. p. 66-68.
30. Lau, K.K.S., J.A. Caulfield, and K.K. Gleason, *Variable angle spectroscopic ellipsometry of fluorocarbon films from hot filament chemical vapor deposition*. *Journal Vac. Sci Technology*, 2000. **18**(5): p. 2404-2411.
31. Livnah, O., et al., *Three-dimensional structures of avidin and the avidin-biotin complex*. *Proc. Natl. Acad. USA*, 1993. **90**: p. 5076-5080.
32. Arsov, L.D., W. Plieth, and G. Kossmehl, *Electrochemical and Raman spectroscopic study of polyaniline; influence of the potential on the degradation of polyaniline.pdf*. *Journal of Solid State Electrochemistry*, 1998. **2**(5): p. 355-361.
33. Bernard, M.C. and A. Hugot-Le Goff, *Quantitative characterization of polyaniline films using Raman spectroscopy*. *Electrochimica Acta*, 2006. **52**(2): p. 595-603.
34. Hsu, S.-M., L. Raine, and H. Fanger, *Use of Avidin-Biotin-Peroxidase Complex(ABC) in Immunoperoxidase Techniques*. *Journal of Histochemistry and Cytochemistry*, 1981. **29**(4): p. 577-580.